

# Effect of Pulsed Radiofrequency with Various Time-Course on Rheumatoid Arthritis Joint Pain in Rats

Xin Li<sup>1,2,\*</sup>, Meng Wang<sup>2,\*</sup>, YingDi Wang<sup>2</sup>, Gang Zhao<sup>3</sup>, Ju Gao<sup>4,5</sup>, Cunjin Wang<sup>4,5</sup>

<sup>1</sup>Department of Clinical Medical College, Yangzhou University, Yangzhou, 225001, People's Republic of China; <sup>2</sup>Department of Anesthesiology, Wuxi Ninth People's Hospital Affiliated to Soochow University, Wuxi, 214063, People's Republic of China; <sup>3</sup>Department of Orthopedics, Wuxi Ninth People's Hospital Affiliated to Soochow University, Wuxi, 214063, People's Republic of China; <sup>4</sup>Department of Anesthesiology, Northern Jiangsu People's Hospital Affiliated to Yangzhou University, Yangzhou, 225001, People's Republic of China; <sup>5</sup>Department of Pain Treatment, Northern Jiangsu People's Hospital Affiliated to Yangzhou University, Yangzhou, 225001, People's Republic of China

\*These authors contributed equally to this work

Correspondence: Cunjin Wang, Email [cunjinwang@163.com](mailto:cunjinwang@163.com)

**Objective:** This study aimed to evaluate the effect of pulsed radiofrequency (PRF) treatment with various time courses on rheumatoid arthritis (RA)-caused joint pain and pathological damage in rats.

**Methods:** SD rats were randomly assigned to five groups: a sham group, an RA group, a PRF/1min group, a PRF/2min group, and a PRF/3min group. RA model rats were established by injecting a mixture of type II collagen and Freund's adjuvant. Four times after 8 weeks, the dorsal root ganglia (DRG) of L4-6 segments were stimulated with PRF for 1, 2, and 3 minutes, respectively. Joint diameters were measured weekly before and after modelling. After 14 days of PRF treatment, morphological changes in cartilage were scored using pathological staining. ELISA determined TNF- $\alpha$ , IL-6, and IL-1 $\beta$  in peripheral blood. Ki67 expression in synovial tissues was detected using immunohistochemistry. Finally, the expression of transient receptor potential ankyrin 1 (TRPA1) and transient receptor potential vanilloid 1 (TRPV1) in synovial tissues were examined by Western blotting, qRT-PCR, and immunofluorescence.

**Results:** Among the RA rats, PRF treatments of 2 minutes and 3 minutes ameliorated joint damage, and both were superior to the 1-minute treatment. Compared to the RA group, the PRF-treated groups showed significantly lower Mankin and OARSI scores, and reduced levels of TNF- $\alpha$ , IL-1 $\beta$ , and IL-6 in peripheral blood. Additionally, there was a decrease in Ki67 expression and levels of TRPA1 and TRPV1 in synovial tissues.

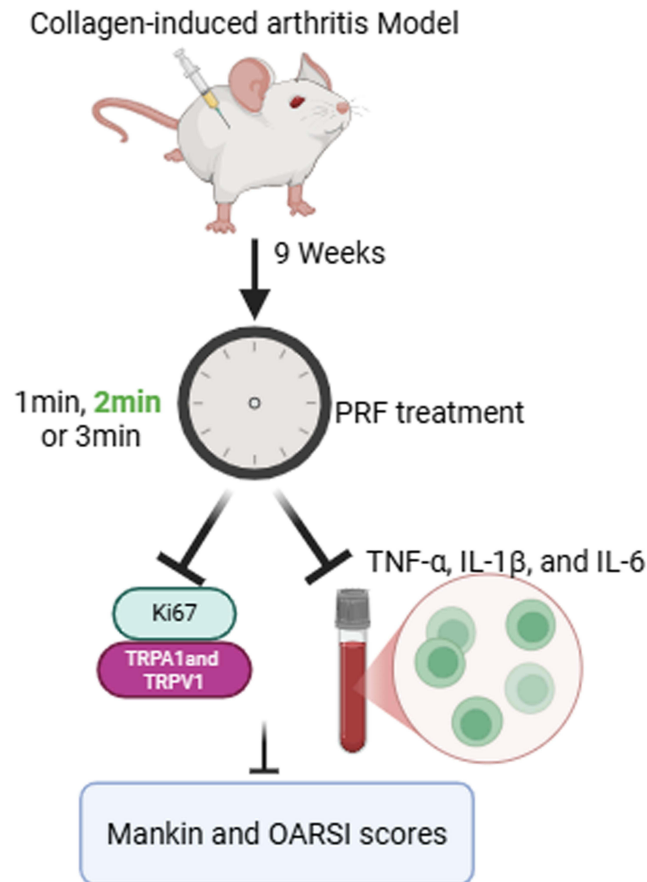
**Conclusion:** RA rats treated with PRF experienced reduced cartilage damage, which appears to be associated with inhibition of joint inflammation.

**Keywords:** pulsed radiofrequency, rheumatoid arthritis, joint damage, TRPA1, TRPV1

## Introduction

Rheumatoid arthritis (RA) is a common immune-mediated inflammatory disease that occurs more frequently in women than in men, particularly among the elderly. Studies indicate that the prevalence of RA ranges from 0.5% to 1% of the general population, depending on regional differences.<sup>1,2</sup> This condition is characterized by inflammation of the synovial membrane and destruction of cartilage,<sup>3</sup> primarily affecting the synovium, tendon sheaths, and synovial bursae in the joints.<sup>4</sup> Symptoms include joint pain and stiffness, swelling, deformity, and impaired function. Current treatment for RA focuses on reducing joint inflammation, swelling, and pain. The most prescribed medications include non-steroidal anti-inflammatory drugs (NSAIDs), glucocorticoids, and disease-modifying antirheumatic drugs.<sup>5</sup> However, it is important to note that these treatments often lack specificity and may require prolonged, high-dose use, leading to significant side effects. Additionally, many patients struggle with compliance due to the complexity and cost of oral, intravenous, and

## Graphical Abstract



intra-articular injections, which often have low bioavailability.<sup>6–8</sup> These challenges highlight the urgent need for safer, more effective, and cost-efficient treatment options for RA.

Pulsed radiofrequency (PRF) is a pain management technique first proposed by Sluiter in 1997.<sup>9</sup> It is widely used in clinical practice for various pain conditions due to its safety, ease of application, and minimal side effects. Several clinical studies suggest that PRF can be applied to many conditions, including small joint lesions, sacroiliac joint lesions, peripheral nerve injuries, postherpetic neuralgia, and cervicogenic headaches. Moreover, PRF treatment can be administered to various sites, such as the dorsal root ganglia, nerve roots, nerve trunks, posterior branches of spinal nerves, and peripheral nerves. Li et al examined the effects of PRF on rats with chronic sciatic nerve compression injuries.<sup>10</sup> The results showed that PRF significantly improved tactile pain sensitivity in these rats.<sup>10</sup> Ma et al demonstrated that PRF treatment effectively alleviates both inflammation and pain responses in a rat model of neuropathic pain, highlighting its potential as a valuable therapeutic option.<sup>11</sup> Furthermore, PRF has also effectively treated conditions involving the suprascapular nerve,<sup>12</sup> the occipital nerve,<sup>13</sup> and other peripheral nerves in clinical practice.<sup>14,15</sup> However, the optimal duration of PRF treatment for RA, its effects on joint pathology, and the underlying mechanisms remain largely unexplored. Therefore, this study was designed to compare the therapeutic effects of different PRF durations (1, 2, and 3 minutes) in a rat model of RA.

Transient receptor potential (TRP) channels are considered potential sensors and transducers of inflammation-related pain.<sup>16</sup> TRPA1 (transient receptor potential ankyrin 1) and TRPV1 (transient receptor potential vanilloid 1) play significant roles in the perception of inflammation and injury in sensory neurons and non-neuronal tissues.<sup>17–19</sup>

TRPV1 is a non-selective calcium channel whose expression and activity significantly rise following DRG inflammatory stimulation, leading to chronic nociceptive sensitization.<sup>20</sup> Furthermore, TRPV1 is also expressed in sensory neurons and nerve terminals within the synovium. It has been demonstrated to mediate peripheral hyperalgesia and is considered a nociceptor in knee osteoarthritis.<sup>21</sup> Similarly, TRPA1 is widely expressed in sensory neurons and non-neuronal cells, including synovium, underscores its relevance to sensory perception and inflammatory processes.<sup>22,23</sup> Extensive research has established a connection between the TRPA1/TRPV1 and inflammation-related pain, highlighting their potential as targets for treating RA.<sup>18</sup> In a significant study by Fu et al, PRF effectively decreased pain sensitivity in rats with chronic constriction injury (CCI).<sup>24</sup> It is possible that one reason for this remarkable outcome may be because inhibitory mechanisms were used to inhibit key chemokines like SDF-1/CXCR4 and TRPV1, along with modulating pro-inflammatory markers like TNF- $\alpha$  and IL-6.<sup>24</sup> Based on this, the expression levels of TRPV1 and TRPA1 in synovial tissue were further examined in this study. The rationale is that the synovium is the primary site of joint inflammation in RA, and that these channels are expressed not only in DRG sensory neurons but also directly in nerve endings and synovial cells within the synovium. By detecting changes in TRPV1 and TRPA1 in synovial tissue, the impact of PRF on local joint pain signaling pathways and peripheral sensitization can be more directly assessed. These compelling findings suggest that PRF could serve as a promising approach to relieving joint pain in RA by effectively suppressing TRPA1 and TRPV1 by reducing inflammation.

In this study, we established a rat model of RA to systematically explore the impact of PRF treatment at varying exposure times. We hypothesize that PRF exerts a duration-dependent analgesic and anti-inflammatory effect in RA rats by suppressing pro-inflammatory factor release and modulating the TRPA1/TRPV1 signaling pathway. Our aims are to: (1) evaluate the effects of different PRF durations on joint pain and tissue damage; (2) examine PRF-mediated changes in pro-inflammatory factor levels; and (3) elucidate the underlying mechanism involving TRPA1/TRPV1 and inflammatory responses, with the ultimate goal of alleviating RA-related joint pain and injury.

## Materials and Methods

### Animals and Surgical Procedures

To ensure the welfare of laboratory animals, all experimental procedures with animals were performed in compliance with the Guide for the Care and Use of Laboratory Animals (National Academies Press, 2011). All animal experiments were approved by Wuxi Ninth People's Hospital Affiliated to Soochow University for Scientific Research's Ethics Committee (Grant number: KS2025020). Sprague Dawley (SD) rats aged 6–8 weeks, provided by Yangzhou University Laboratory Animal Center, were of clean-grade and healthy. During the experiment, rats were maintained at 22 $\pm$ 2 °C, 50–60% humidity, 12-hour cycles of daylight and darkness, and sufficient food and water was available.

The model was established using the collagen-induced arthritis (CIA) method, a reliable approach to studying the disease. Initially, all rats were acclimatized and kept for one week to ensure their readiness. The mixture inducer for the RA rat model was prepared by thoroughly mixing equal parts of 4 mg/mL bovine type II collagen (C7806, Sigma, USA) and 4 mg/mL complete Freund's adjuvant (CFA) (F5881, Sigma, USA). Following this, the rats were anesthetized with isoflurane, and a 100  $\mu$ L dose of this induced mixture was injected subcutaneously at multiple sites on the first day, with an additional immunization dose after one week to reinforce the response. The model typically becomes evident within 3 to 7 days. In contrast, the Sham group received the same volume of saline to serve as a control.

### PRF Treatment

SD rats were randomly assigned to five groups: Sham, RA, PRF/1 min, PRF/2 min, and PRF/3 min, with six animals in each group. A random number table was used for randomization, and the allocation sequence was generated by an independent researcher. On the first day of the ninth week following the RA model construction, the rats were carefully anesthetized by inhaling 1% isoflurane. A trocar needle was strategically inserted at the location of the DRG in the L4-6 segments of each rat. After the trocar was removed, PRF stimulation electrodes were precisely placed. The animals designated for the PRF treatment group received targeted stimulation using a 20 Hz pulse frequency current at a controlled temperature of 42°C, provided by a reliable radiofrequency lesion generator (R2000B, Beijing Neo

Science Co., Ltd, Beijing, China). PRF/1 min, PRF/2 min, and PRF/3 min groups were experienced by stimulation for varying durations of 1 minute, 2 minutes, and 3 minutes, respectively. Each rat received one PRF treatment every 20 minutes, for a total of four treatments. The investigator who performed the PRF treatment was blinded to the group allocation. The blinding code was revealed only after all experimental procedures and data collection were completed. In brief, each animal was placed in a transparent sealed euthanasia chamber, and CO<sub>2</sub> was gradually introduced at a moderate flow rate until a concentration of 60–70% was reached, to minimize distress caused by rapid gas flow. Euthanasia was performed until respiratory arrest and absence of the corneal reflex were confirmed, after which CO<sub>2</sub> exposure was maintained for an additional 1–2 minutes to ensure that death was irreversible and to minimize animal distress.

## Joint Swelling Test and Pain Threshold Measurement

Since the beginning of RA rat modeling, ankle diameters have been measured weekly using vernier calipers and statistically analyzed.

To assess all rats' pain threshold accurately, we measured tail-flick latency in a hot water bath on days 1, 3, 7, 10, and 14 following PRF treatment. The process began when 1/3 of the rat's tail was immersed in a 48°C-water bath, and timing commenced. It stopped when the rat instinctively removed its tail from the water, marked by tail wagging or curling. This reaction time was recorded as tail-flick latency. Each rat underwent this measurement three times, with at least 20 minutes intervals between each test to ensure reliability. The average latency was calculated from these three measurements.

## Histological Evaluation of RA

To effectively assess RA severity, we carefully isolated the femoral condyle and tibial plateau on the operative side. We then fixed these tissues in a 4% (vol/vol) paraformaldehyde solution (P1110, Solarbio, Beijing, China). Following this critical step, we performed decalcification using a 0.5M EDTA solution (E1170-100, Solarbio, Beijing, China). After thoroughly dehydrating the specimens through a progressive alcohol gradient, we embedded the decalcified tissues in paraffin and sectioned them into 5- $\mu$ m slides. These sections were prepared in both the coronal plane at the midpoint of the tibial plateau and the sagittal plane at the midpoint of the medial femoral condyle. We then applied H&E staining (PK10031, Proteintech, Wuhan, China) and Safranin O/fast green staining (G1053, Servicebio, Wuhan, China) to the sections. We utilized both the Osteoarthritis Research Society International (OARSI) grading system and the Mankin grading system to evaluate RA severity. The Mankin scoring system is crucial for evaluating RA severity. It comprehensively examines vital aspects such as cartilage structure, chondrocyte health, cartilage matrix staining, and tidemark integrity. Scores range from 0 to 14, with higher numbers indicating increased severity. The OARSI bone damage assessment criteria were evaluated as previously described.<sup>25</sup> To enhance the reliability of our findings, three colleagues independently assessed RA severity in a blind manner.

## Enzyme Linked Immunosorbent Assay (ELISA)

Before euthanizing the rats, a blood sample was taken from the abdominal aorta. Then, the blood sample was rested at room temperature (20–25 °C) for 1 hour. Afterward, the upper layer of serum was separated by centrifugation at 3000 RPM for 10 minutes. The levels of pro-inflammatory factors, including TNF $\alpha$ , IL-6, and IL-1 $\beta$ , were measured in peripheral blood following the instructions provided with the ELISA kit (E-EL-R0015, Elabscience, Wuhan, China).

## Western Blotting

The total protein extracts from each sample were prepared using RIPA lysis buffer (P0013B, Beyotime, Shanghai, China). Following 10-minute centrifugation, the supernatant was collected, and the protein concentration was measured using a BCA protein assay kit (P0009, Beyotime, Shanghai, China). For sodium dodecyl sulfate-polyacrylamide gel electrophoresis (SDS-PAGE), 20 $\mu$ g of protein per sample was separated and transferred to PVDF membranes (Millipore, Billerica, MA, USA). The membranes were blocked with 5% milk in TBST-20 for 1 hour at room temperature. They were then incubated overnight at 4°C with primary antibodies targeting TRPA1 (19,124-1-AP, Proteintech, USA) and TRPV1 (66,983-1-Ig, Proteintech, USA) After a rinse with TBST, the blots were incubated with goat anti-rabbit IgG

**Table 1** Gene-Specific Primer Sequences Used for qRT-PCR

<i>TRPA1</i>	Forward primer	ATGAGTTGGCATACCCGGTC
	Reverse primer	CCACTTTGCGCAAGTACCAG
<i>TRPV1</i>	Forward primer	GGCCGAGTTTCAGGGAGAAA
	Reverse primer	GGTCCCTAAGCAGACCACC
<i>β-actin</i>	Forward primer	CACCCGCGAGTACAACCTTC
	Reverse primer	CCCATACCCACCATCACACC

conjugated with peroxidase (1:5000 dilution; CST, USA). A rabbit anti-actin antibody (1:5000, CST, USA) was used as a loading control to ensure equal protein loading across samples. Data analysis was performed using a ChemiDoc XRS Plus luminescent image analyzer (Bio-Rad, USA), following enhancement with chemiluminescence reagents (36222ES60, Yeasen, Shanghai, China).

### Quantitative Real-Time PCR (qRT-PCR) Analysis

Total RNA was extracted from each sample using TRIzol reagent (R0016, Beyotime, Shanghai, China). One µg of total RNA was reverse-transcribed for each sample into single-stranded cDNA using the 2×Q3 SYBR qPCR Master Mix (Universal) kit (KCD-M1004, Cronda, Shanghai, China). Quantitative real-time PCR (qRT-PCR) was performed with the HiScript II QRT SuperMix for qPCR kit (R222, Vazyme, Nanjing, China) on a real-time PCR system (5200multi, Tanon, Shanghai, China), which was employed to process and analyze all reactions. Relative gene expression levels were calculated using the  $2^{-\Delta\Delta C_t}$  method, with target gene expression normalized to  $\beta$ -actin. Table 1 shows the primer sequences for qRT-PCR.

### Immunohistochemistry and Immunofluorescence

For immunohistochemistry, paraffin sections were deparaffinized sequentially using xylene, followed by a gradient of alcohol, and then rehydrated in distilled water for 5 minutes. The tissue sections were placed in a repair cassette filled with citrate antigen retrieval solution (Beyotime) and subjected to microwave heating for antigen retrieval. After allowing the slides to cool naturally, they were placed in PBS (pH 7.4) on a decolorizing shaker and washed by shaking three times for 5 minutes each. At room temperature, 3% hydrogen peroxide was incubated for 15 minutes to inactivate endogenous peroxidase activity. Next, the sections were permeabilized with 0.3% Triton X-100 for 30 minutes, blocked with 5% BSA for 1 hour, and immunolabeled overnight with Ki67 (ab15580, Abcam, USA) antibodies. Next, following the manufacturer's instructions, we conducted Ki67 staining on the synovial tissues of rats in each group using the Universal Rabbit Two-Step Assay Kit (PV-900) from ZSGB-BIO (Beijing, China).

For immunofluorescence, after the antigen retrieval, the sections were permeabilized with 0.3% Triton X-100 for 30 minutes, blocked with 5% BSA for 1 hour, and then immunolabeled overnight with TRPA1 (19,124-1-AP, Proteintech, USA) and TRPV1 (66,983-1-Ig, Proteintech, USA) antibodies. The sections were rewashed with PBS and incubated with the goat anti-rabbit IgG H&L (ab6939, Abcam, USA) or goat anti-mouse IgG H&L (ab6785, Abcam, USA) secondary antibody at room temperature for 1.5 hours. Finally, the sections were mounted using Fluoroshield with DAPI (GeneTex Inc. USA). Every sample was examined using fluorescence microscopy (DMI1, Leica, Germany). The resulting images were then quantified with ImageJ software for comprehensive data analysis. Quantification of histological staining was performed by an independent investigator who was blinded to the experimental groups.

### Statistical Analysis

All data were analyzed and plotted using GraphPad Prism 9.0 software. Measurement data were assessed for normal distribution, including Mankin and OARSI scores, inflammatory cytokines, Ki67-positive expression, TRPA, TRPV1, and related protein expressions. Following this test, those with a normal distribution were expressed as mean ± standard deviation. Analysis was conducted using a one-way ANOVA with Tukey's post-hoc test. Multifactorial ANOVA

examined differences in ankle diameters and pain thresholds among different groups with Tukey’s post-hoc test. A two-sided Alpha level of 0.05 was established for statistical significance.

## Results

### PRF Treatment Improves Joint Pain and Histopathology in RA Rats

The ankle diameter measurements in each group of rats demonstrated that the RA group had significantly larger ankle diameters than the sham group ( $11.30 \pm 0.53$  mm vs.  $8.98 \pm 0.37$  mm), confirming the successful establishment of the RA model. Remarkably, after administering PRF treatment, we observed a significant reduction in the ankle diameters of the RA rats (Figure 1A). This compelling evidence suggests that localized PRF treatment effectively mitigates joint swelling in RA rats and has preliminarily confirmed its promising therapeutic potential. Moreover, the behavioral tests revealed that the PRF-treated group displayed remarkably longer tail-flick latencies compared to the RA group on days 7 to 14

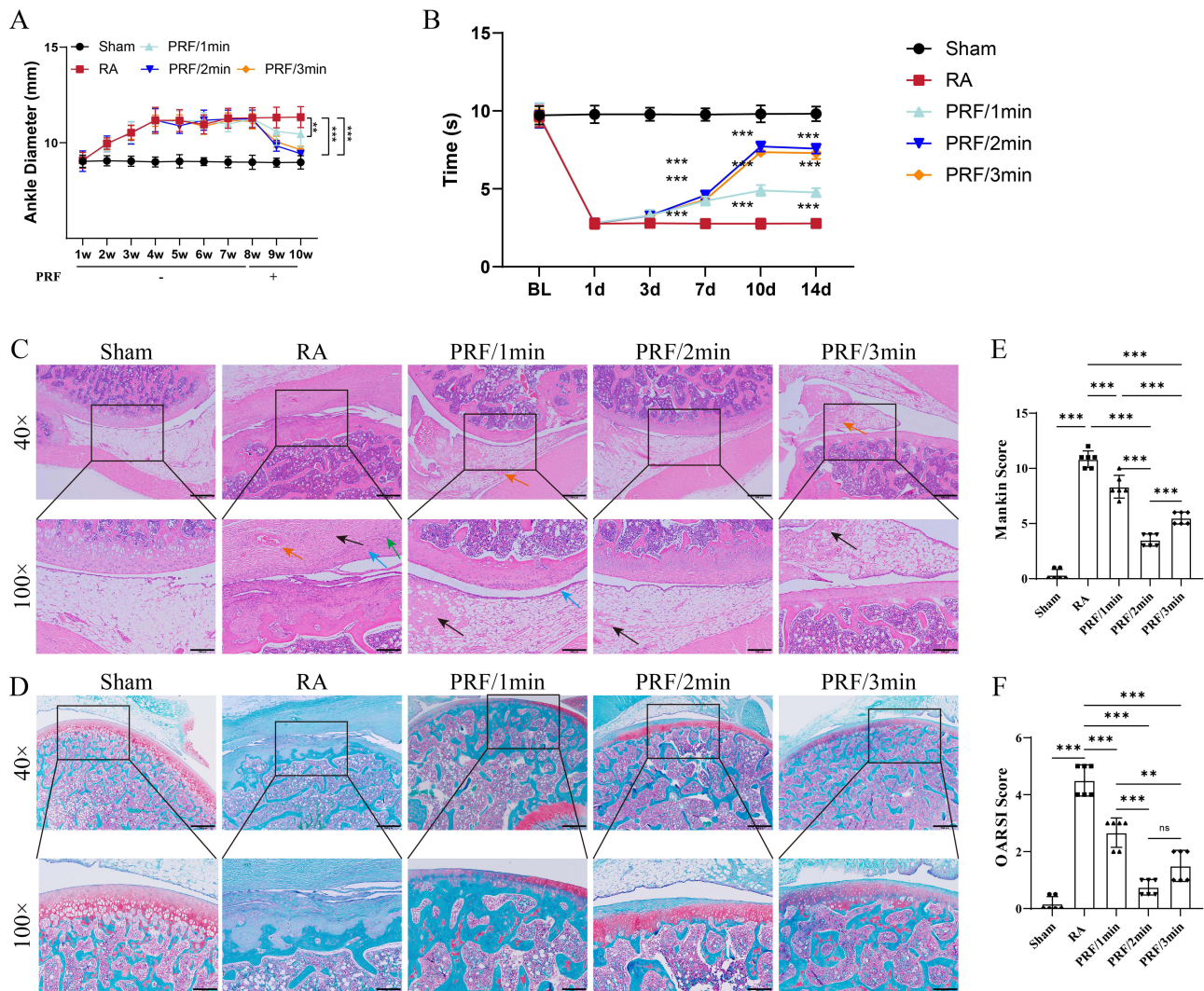


**Figure 1** PRF treatment improves joint pain and histopathology in RA rats. **(A)** Measure the ankle diameters of each group in an RA rat model.  $n=6$  per group. “-” indicates that PRF treatment was not administered; “+” indicates that PRF treatment was administered at week 9 (Interaction:  $F(36, 250) = 5.927, P < 0.001$ ;  $n=6$  per group). **(B)** Latency of tail-flick of each group in an RA rat model (Interaction:  $F(20, 150) = 80.95, P < 0.001$ ;  $n=6$  per group). BL: baseline. **(C)** Representative images of H&E staining of rat osteoarticular joints in each group, with blue arrows representing synovial cell hyperplasia, black arrows representing proliferation of the underlying sponged fibrous tissues, Orange arrows representing vascular hyperplasia, and green arrows representing lymphocytic infiltration. Scale bar,  $500\mu\text{m}$  ( $4\times$ ) and  $200\mu\text{m}$  ( $100\times$ ).  $n=6$  per group. **(D)** Representative images of SOFG staining of osteoarticular joints of each group in an RA rat model. Scale bar,  $500\mu\text{m}$  ( $4\times$ ),  $200\mu\text{m}$  ( $100\times$ ).  $n=6$  per group. **(E-F)** Arthritis severity was assessed in each group using the Mankin and OARSI scoring systems (Mankin  $F(4, 25) = 200.9, P < 0.001$ ; OARSI  $F(4, 25) = 88.02, P < 0.001$ ;  $n=6$  per group). \*\* $P < 0.01$ , \*\*\* $P < 0.001$ . ns, no statistical difference. For comprehensive information, please refer to [Table S1](#).

after treatment. Notably, the PRF/2min and PRF/3min group outperformed the PRF/1min group, achieving even greater tail-flick latencies (Figure 1B).

Moreover, histopathological evaluation revealed that the RA group displayed typical characteristics of joint destruction. These included abnormal synovial hyperplasia with inflammatory cell infiltration and significant degeneration of the articular cartilage when compared to the Sham group. H&E staining analysis indicated an increase in synovial lining thickness, accompanied by fibrous tissue hyperplasia in the lower layer, an enlarged area of vascular neovascularization, and a higher density of lymphocyte infiltration in the RA group in comparison to the Sham group (Figure 1C). These findings reflect an active inflammatory state in the RA model (Figure 1D). Additionally, SOFG staining analysis showed proteoglycan depletion in the articular cartilage of the RA group, characterized by diminished staining intensity compared to the Sham group (Figure 1D), further confirming the severe destruction of the cartilage matrix. Notable, PRF intervention effectively improved the previously mentioned arthropathic injuries by reducing the synovial hyperplasia index, inflammatory cell infiltration, and partially restoring cartilage proteoglycan content (Figure 1C and D).

Furthermore, we used the Mankin and OARSI scoring systems to objectively evaluate the effects of PRF treatment. Our results showed that the articular cartilage structure remained intact in the Sham group. In contrast, the RA group exhibited significantly higher scores (Figure 1E and F), indicating severe damage caused by the RA models. Meanwhile, the scores for the PRF-treated groups were significantly lower than those for the RA group ( $P < 0.05$ ), suggesting that PRF treatment helps mitigate articular cartilage destruction. Notably, the PRF/2 min and PRF/3 min groups were more effective than the PRF/1 min group in relieving joint pain and improving the pathological symptoms of arthritis.

Based on these results, we conclude that the established rat model of RA possesses a typical arthritic phenotype, that PRF treatment reduces damage to articular cartilage in RA, and that longer periods of PRF treatment result in superior results.

## PRF Treatment Inhibits RA-Related Inflammation and Synovial Hyperproliferation

To further investigate whether the PRF treatment influences inflammation resulting from RA and synovial proliferation, we evaluated the levels of the pro-inflammatory factor in peripheral blood using ELISA and the expression of Ki67 in synovium using immunohistochemistry. The ELISA results indicated that the pro-inflammatory cytokines TNF- $\alpha$ , IL-6, and IL-1 $\beta$  expression levels in the PRF-treated group's peripheral blood were significantly lower than those in the RA group. Moreover, the reduction of pro-inflammatory factors was more pronounced in the PRF/2min and PRF/3min groups (Figure 2A). These results indicate that PRF treatment can significantly inhibit the activation of pro-inflammatory cytokine networks in the RA rat model.

Furthermore, the immunohistochemical analysis provides critical insights, revealing that the positivity rate of the synovial hyperproliferation marker Ki67 was significantly higher in the RA group versus the Sham group. In contrast, Ki67 expression in RA rats was notably suppressed in the PRF/2min and PRF/3min groups, surpassing the effects seen in the PRF/1min group (Figure 2B). These findings advocate that PRF treatment reduces synovial hyperproliferation and minimizes cartilage damage in RA.

## PRF Treatment Improves Joint Pain and Histopathology via Inhibiting the TRPA1 and TRPV1 Expressions

To further identify the key factors that contribute to improving joint pain and reducing cartilage damage, we performed Western blotting and qPCR analyses to assess the levels of TRPA1 and TRPV1 in synovium from RA rats. Western blot and qPCR analyses demonstrate that the expression levels of TRPA1 and TRPV1 are abnormally elevated in the synovial tissues of RA rats compared to the Sham group (Figures 3A and B). Moreover, PRF intervention led to a significant reduction in the expression levels of these proteins, with the 2-minute and 3-minute PRF treatments showing more pronounced inhibitory effects than the 1-minute treatment (Figures 3A and B).

Additionally, immunofluorescence results further demonstrated spatial co-localization of TRPA1 and TRPV1 in the synovial tissues, suggesting a potential interaction or synergistic relationship between these two channels at the intracellular level. Furthermore, PRF treatment significantly reduced the expression of TRPA1 and TRPV1 in RA rats

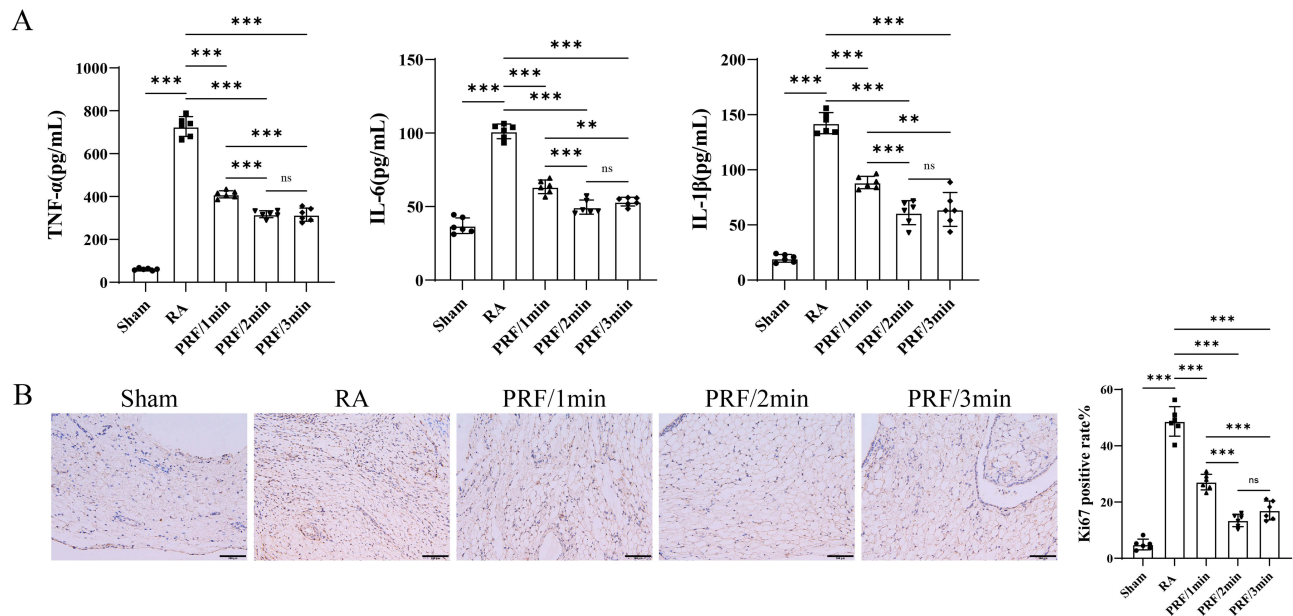


**Figure 2** PRF treatment inhibits RA-related inflammation and synovial hyperproliferation. **(A)** Expression of pro-inflammatory factors, including TNF- $\alpha$ , IL-6 and IL-1 $\beta$  in peripheral blood detected by ELISA in an RA rat model (TNF- $\alpha$ :  $F(4, 25) = 468.9, P < 0.001$ ; IL-6:  $F(4, 25) = 167.7, P < 0.001$ ; IL-1 $\beta$ :  $F(4, 25) = 123.9, P < 0.001$ ;  $n = 6$  per group). **(B)** Representative images of Ki67 staining in synovial tissues for each group ( $F(4, 25) = 153.9, P < 0.001, n = 6$  per group). Scale bar, 100 $\mu$ m. \*\* $P < 0.01$ , \*\*\* $P < 0.001$ , ns, no statistical difference. For comprehensive information, please refer to [Table S2](#).

(Figure 3C). These findings suggest that PRF may function as a powerful analgesic and anti-inflammatory agent by modulating the expression dynamics of TRPA1 and TRPV1 channels in the synovium.

## Discussion

In this study, we successfully established a rat model for RA and revealed that PRF treatments significantly alleviate joint pain and attenuate cartilage damage in RA. Our findings indicate that different PRF treatment regimens can lead to diverse outcomes, such as reducing joint pain, inhibiting synovial hyperproliferation, and reducing cartilage destruction. Additionally, we explored the mechanisms of PRF treatments, which include lowering inflammatory factor levels and downregulating TRPA1 and TRPV1 expression in synovial tissues. These results lay an important experimental foundation for using PRF in chronic inflammatory diseases and highlight TRPA1 and TRPV1 as promising targets for future RA treatments.

RA is a debilitating chronic autoimmune disease characterized by joint inflammation and synovial tissue proliferation. Continuous immune cell activation induced by RA-specific autoantigens causes chronic joint inflammation and swelling of the synovium.<sup>3</sup> This inflammatory environment further promotes the formation of vascular opacities that erode the periarticular bone at the cartilage-bone junction, ultimately resulting in bone erosion and cartilage degeneration.<sup>26</sup> Therefore, modifying the inflammatory environment within the joints is a crucial strategy for treating RA effectively.

In the present study, we utilized the collagen-induced arthritis (CIA) method to create a reliable rat model of RA. The ankle diameters and tail-flick latency of the rats exposed to CIA were significantly larger and shorter than those of the unexposed rats. Furthermore, RA dramatically alters joint health, leading to destruction. Key histopathological features include increased synovial lining thickness, followed by fibrous tissue hyperplasia in the underlying layers. Additionally, there is an increase in neovascularization, a higher concentration of lymphocyte infiltration, and a concerning depletion of proteoglycans in the articular cartilage.<sup>3,27</sup> These changes highlight the severe impact of RA on joint integrity and function.<sup>3,27</sup> In our study, the histological evaluation clearly demonstrated that CIA-treated rats showed distinct signs of joint destruction, with their Mankin and OARSI scores substantially surpassing those of the untreated rats. These above substantial differences demonstrate that we successfully established the RA rat model, as joint swelling and pain sensitivity are typical characteristics of RA.

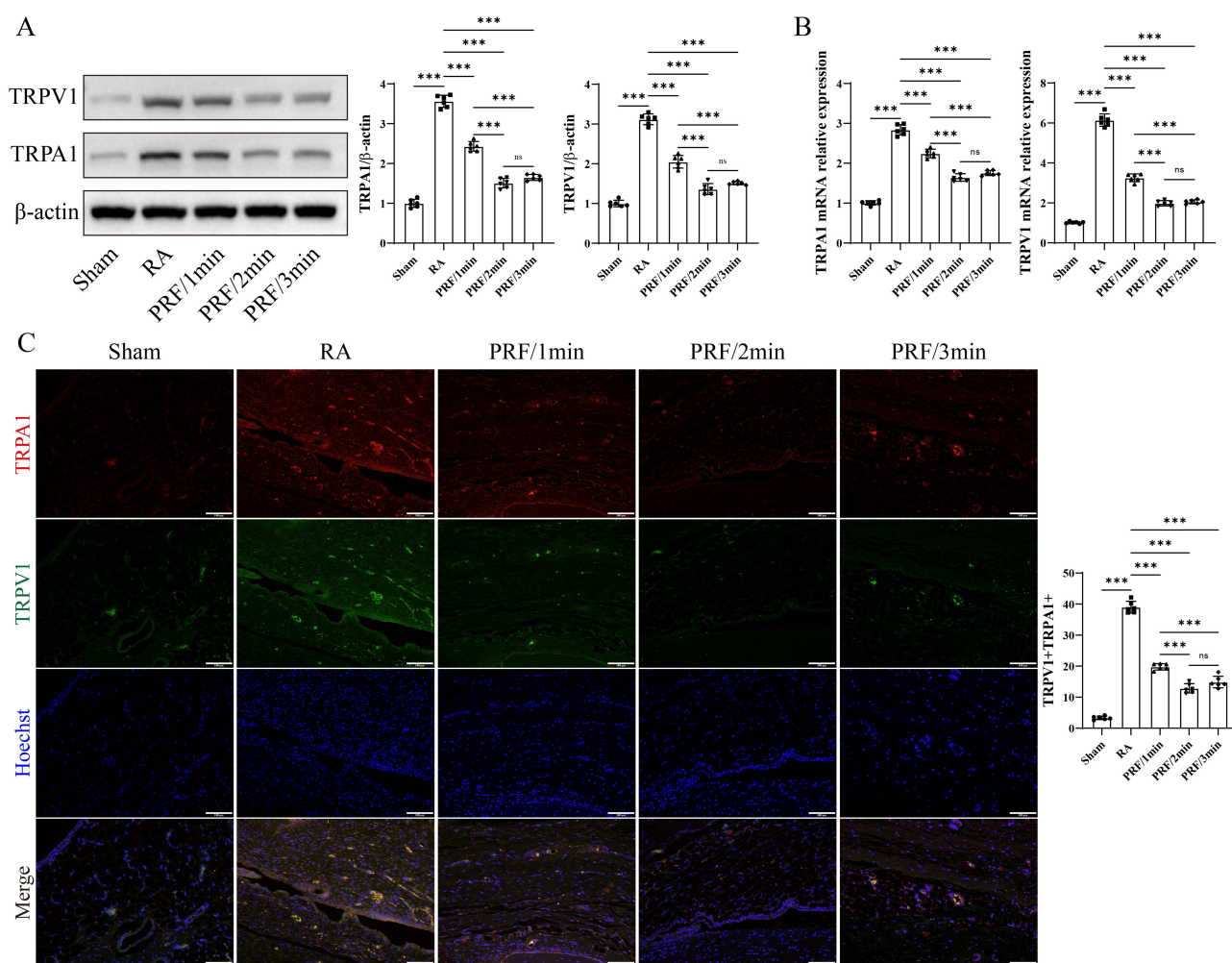


**Figure 3** PRF treatment improves joint pain and histopathology via inhibiting the TRPA1 and TRPV1 expressions. **(A)** Western blotting analysis of TRPV1 and TRPA1 expressions in synovial tissues of an RA rat model for each group (TRPV1:  $F(4, 25) = 289.7, P < 0.001$ ; TRPA1:  $F(4, 25) = 438.7, P < 0.001$ ;  $n = 6$  per group). **(B)** qRT-PCR analysis of the mRNA levels of TRPV1 and TRPA1 expressions in synovial tissues of an RA rat model for each group (TRPV1:  $F(4, 25) = 714.7, P < 0.001$ ; TRPA1:  $F(4, 25) = 317.1, P < 0.001$ ;  $n = 6$  per group). **(C)** Immunofluorescence images of TRPV1 and TRPA1 in synovial tissues of an RA rat model for each group ( $F(4, 25) = 490.9, P < 0.001$ ;  $n = 6$  per group). Scale bar, 100 $\mu$ m. \*\*\* $P < 0.001$ , ns, no statistical difference. For comprehensive information, please refer to [Table S3](#).

Next, we then investigated the potential of PRF in reducing joint swelling and pain associated with RA. Our findings demonstrated that RA rats treated with PRF experienced a significant decrease in ankle size and a longer tail-flick latencies in response to pain, indicating that PRF treatment effectively alleviates joint swelling and reduces pain sensitivity related to RA. This was also validated by the results of histological evaluation, which showed PRF intervention effectively improved the previously mentioned arthropathic injuries by reducing the synovial hyperplasia index, inflammatory cell infiltration, and partially restoring cartilage proteoglycan content. Moreover, the Mankin and OARSI scoring systems also revealed the PRF-treated groups were significantly lower than those for the unexperienced PRF. Further, the levels of the pro-inflammatory factor in peripheral blood were detected using ELISA to assess the RA-caused inflammation. The results showed that the levels of IL-1 $\beta$ , TNF- $\alpha$ , and IL-6 were significantly decreased after PRF treatment in an RA rat model. Abnormal synovial proliferation is one of the most significant pathological features associated with RA due to its strong erosive and destructive effects on cartilage tissue.<sup>3,27</sup> Therefore, we carried out an immunohistochemical analysis to evaluate Ki67 expression, an essential marker of cell proliferation, in synovial tissue. Our findings reveal that PRF treatment markedly reduced the positivity rate of Ki67 in the RA rat mode. These above results demonstrate that PRF treatment may be a powerful strategy for inhibiting the joint inflammatory response, relieving joint pain, and promoting the repair of articular cartilage damage in RA model rats.

Clinical trials involving PRF for longer than two minutes are uncommon.<sup>28–30</sup> Tanaka et al have reported a dose-dependent enhancement of antinociceptive sensitization when PRF duration was extended from 2 to 6 minutes in a resin toxin model with rats.<sup>31</sup> However, Ozsoylar et al found no statistically significant difference in antinociceptive effects between 2-minute and 6-minute PRF applications in a sciatic ligation model.<sup>32</sup> Therefore, the optimal duration for PRF exposure is still not well established and often varies in clinical settings. We evaluated the effects of 1-minute, 2-minute, and 3-minute PRF treatments in the RA rat model to address this issue. Our results indicated that the therapeutic effectiveness of the 2-minute and 3-minute PRF groups was significantly greater than that of the 1-minute group. However, no statistically significant difference was observed between the 2-minute and 3-minute PRF groups. This finding suggests the existence of a physiological saturation point in this model: a stimulation duration of 2 minutes may already achieve maximal suppression of DRG neuronal hyperexcitability and downstream neurogenic inflammation, such that extending treatment to 3 minutes confers no additional benefit. These results suggest that, in the rat RA model, using PRF stimulation for either 2 or 3 minutes may provide superior therapeutic benefits compared to a brief 1-minute exposure.

Recent investigations have underscored the pivotal roles of TRPA1 and TRPV1 channels in mediating inflammation.<sup>33</sup> Atoyan et al revealed that TRPA1 plays a crucial role in regulating the expression of inflammation-related genes in keratinocytes, notably by enhancing the production of IL-1 $\alpha$  and IL-1 $\beta$ .<sup>34</sup> Additionally, exposure of keratinocytes to capsaicin or UV radiation triggers a TRPV1-mediated influx of Ca<sup>2+</sup>, resulting in increased levels of inflammatory factors such as IL-1 $\beta$ , IL-2, IL-4, IL-8, and TNF- $\alpha$ .<sup>35</sup> Thus, activating TRPA1 and TRPV1 is a clear pathway to amplifying the inflammatory response. In our current study, we utilized Western blotting and qPCR techniques to assess the impact of PRF treatment on the expression of TRPA1 and TRPV1 in synovial tissues in an RA rat model. Our findings indicate that PRF treatment effectively inhibits the expression of TRPA1 and TRPV1 in RA-induced swollen synovial tissues. It is worth noting that although PRF acts on DRG distant from the knee joint, its effect on synovial TRP channels is likely mediated through modulation of sensory neuron activity and subsequent alterations in peripheral neurogenic inflammation.<sup>36</sup> By inhibiting the secretion of calcitonin gene-related peptide (CGRP) and substance P (SP) into the knee joint due to impaired axonal transport in DRG neurons,<sup>37</sup> PRF reduces the levels of pro-inflammatory cytokines, which are key mediators of inflammation and pain.<sup>38</sup> Furthermore, immunofluorescence analyses confirmed the spatial co-localization of TRPA1 and TRPV1 within these tissues, suggesting a potential interaction or synergistic relationship between these two channels at the intracellular level. Collectively, these results strongly support the notion that reduced TRPA1 and TRPV1 expression is associated with the alleviation of inflammatory responses in RA following PRF treatment, presenting a promising therapeutic strategy for managing this debilitating condition.

Our previous study clearly demonstrated that targeting the DRG with PRF results in significantly greater analgesia than intra-articular PRF, by effectively downregulating TRPA1/TRPV1 channels and reducing inflammatory factors.<sup>39</sup> Building on this critical finding, the current study focuses on determining the optimal PRF duration at this crucial site (DRG). By creating groups with PRF durations of 1, 2, and 3 minutes, we address the critical issue of PRF parameter optimization, thereby enhancing the clinical applicability of the protocol. Furthermore, by evaluating the synovial proliferation marker Ki67, performing quantitative cartilage damage assessments using the Mankin and OARSI scales, and conducting Safranin O/Fast Green staining, we expand our evaluation beyond mere pain relief to include histopathological repair. This comprehensive approach enables more thorough validation of therapeutic efficacy, underscoring the potential impact of our findings.

The current study presents compelling insights but also highlights important limitations: (1) The effects of PRF were assessed over a brief 14-day period. Considering the slow improvement in joint pain and damage associated with RA, it's clear that continued observation over a more extended timeline is essential for understanding long-term benefits. (2) The tail flick test measures nociceptive reflex rather than joint-specific pain; future studies should include von Frey testing or weight-bearing asymmetry for mechanical allodynia to better characterize arthritis-related pain. (3) While this study suggests that PRF may enhance joint symptoms in RA by inhibiting the expression of TRPA1 and TRPV1, the underlying mechanisms remain unclear. A deeper exploration into how PRF provides analgesic effects is crucial for validating its efficacy. (4) Moreover, future investigations are vital to identify the optimal parameters for PRF therapy, enabling more effective treatment strategies. Addressing these limitations will enhance the understanding and application of PRF therapy in managing RA.

## Conclusion

PRF treatment ameliorated joint swelling and pain, decreased inflammatory factors released, inhibited synovial proliferation, and reduced cartilage damage via inhibiting synovial TRPA1/TRPV1 expression in an RA rat model. Moreover, PRF treatment with various exposure durations showed differential therapeutic effects; the 2-minute PRF treatment proved to be more effective overall.

## Data Sharing Statement

The data that support the findings of this study are available from the corresponding author upon reasonable request.

## Ethics Approval and Consent to Participate

All experimental procedures with animals were approved by Wuxi Ninth People's Hospital Affiliated to Soochow University for Scientific Research's Ethics Committee (Grant number: KS2025020).

## Author' Contributions

All authors made a significant contribution to the work reported, whether that is in the conception, study design, execution, acquisition of data, analysis and interpretation, or in all these areas; took part in drafting, revising or critically reviewing the article; gave final approval of the version to be published; have agreed on the journal to which the article has been submitted; and agree to be accountable for all aspects of the work.

## Funding

This study was supported by the National Natural Science Foundation of China (82171207), the Natural Science Foundation of Jiangsu Province (BK20231246) and the Youth Excellent Talent Training Project of "333" High-Level Personnel Training Program in Jiangsu Province (2022-3-6-146).

## Disclosure

The authors declare that there is no conflicts of interest regarding the publication of this paper.

## References

- Cao Y, Yang Y, Hu Q, Wei G. Identification of potential drug targets for rheumatoid arthritis from genetic insights: a Mendelian randomization study. *J Transl Med.* 2023;21(1):616. doi:10.1186/s12967-023-04474-z
- Silman AJ, Pearson JE. Epidemiology and genetics of rheumatoid arthritis. *Arthritis Res.* 2002;4(3):S265–72. doi:10.1186/ar578
- Smolen JS, Aletaha D, McInnes IB. Rheumatoid arthritis. *Lancet.* 2016;388(10055):2023–2038. doi:10.1016/S0140-6736(16)30173-8
- Sharif K, Sharif A, Jumah F, Oskouian R, Tubbs RS. Rheumatoid arthritis in review: clinical, anatomical, cellular and molecular points of view. *Clin Anat.* 2018;31(2):216–223. doi:10.1002/ca.22980
- Burmester GR, Pope JE. Novel treatment strategies in rheumatoid arthritis. *Lancet.* 2017;389(10086):2338–2348. doi:10.1016/S0140-6736(17)31491-5
- Shreya AB, Raut SY, Managuli RS, Udupa N, Mutalik S. Active targeting of drugs and bioactive molecules via oral administration by ligand-conjugated lipidic nanocarriers: recent advances. *AAPS PharmSciTech.* 2018;20(1):15. doi:10.1208/s12249-018-1262-2
- Anil U, Markus DH, Hurley ET, et al. The efficacy of intra-articular injections in the treatment of knee osteoarthritis: a network meta-analysis of randomized controlled trials. *Knee.* 2021;32:173–182. doi:10.1016/j.knee.2021.08.008
- McNicol ED, Ferguson MC, Schumann R. Single-dose intravenous diclofenac for acute postoperative pain in adults. *Cochrane Database Syst Rev.* 2018;8(8):CD012498. doi:10.1002/14651858.CD012498.pub2
- De la Cruz J, Benzecry Almeida D, Silva Marques M, Ramina R, Fortes Kubiak RJ. Elucidating the mechanisms of pulsed radiofrequency for pain treatment. *Cureus.* 2023;15(9):e44922. doi:10.7759/cureus.44922
- Li DY, Meng L, Ji N, Luo F. Effect of pulsed radiofrequency on rat sciatic nerve chronic constriction injury: a preliminary study. *Chin Med J.* 2015;128(4):540–544. doi:10.4103/0366-6999.151113
- Ma KH, Cheng CY, Chan WH, et al. Pulsed radiofrequency upregulates serotonin transporters and alleviates neuropathic pain-induced depression in a spared nerve injury rat model. *Biomedicines.* 2021;9(10). doi:10.3390/biomedicines9101489
- Gofeld M, Restrepo-Garces CE, Theodore BR, Faclier G. Pulsed radiofrequency of suprascapular nerve for chronic shoulder pain: a randomized double-blind active placebo-controlled study. *Pain Pract.* 2013;13(2):96–103. doi:10.1111/j.1533-2500.2012.00560.x
- Choi HJ, Oh IH, Choi SK, Lim YJ. Clinical outcomes of pulsed radiofrequency neuromodulation for the treatment of occipital neuralgia. *J Korean Neurosurg Soc.* 2012;51(5):281–285. doi:10.3340/jkns.2012.51.5.281
- Choi GS, Ahn SH, Cho YW, Lee DG. Long-term effect of pulsed radiofrequency on chronic cervical radicular pain refractory to repeated transforaminal epidural steroid injections. *Pain Med.* 2012;13(3):368–375. doi:10.1111/j.1526-4637.2011.01313.x

15. Lim SM, Park HL, Moon HY, et al. Ultrasound-guided infraorbital nerve pulsed radiofrequency treatment for intractable postherpetic neuralgia - a case report. *Korean J Pain*. 2013;26(1):84–88. doi:10.3344/kjp.2013.26.1.84
16. Kameda T, Zvick J, Vuk M, et al. Expression and activity of TRPA1 and TRPV1 in the intervertebral disc: association with inflammation and matrix remodeling. *Int J Mol Sci*. 2019;20(7):1767. doi:10.3390/ijms20071767
17. Marrone MC, Morabito A, Giustizieri M, et al. TRPV1 channels are critical brain inflammation detectors and neuropathic pain biomarkers in mice. *Nat Commun*. 2017;8:15292. doi:10.1038/ncomms15292
18. Fernandes ES, Fernandes MA, Keeble JE. The functions of TRPA1 and TRPV1: moving away from sensory nerves. *Br J Pharmacol*. 2012;166(2):510–521. doi:10.1111/j.1476-5381.2012.01851.x
19. Kelly S, Chapman RJ, Woodhams S, et al. Increased function of pronociceptive TRPV1 at the level of the joint in a rat model of osteoarthritis pain. *Ann Rheum Dis*. 2015;74(1):252–259. doi:10.1136/annrheumdis-2013-203413
20. Yu L, Yang F, Luo H, et al. The role of TRPV1 in different subtypes of dorsal root ganglion neurons in rat chronic inflammatory nociception induced by complete Freund's adjuvant. *Mol Pain*. 2008;4:61. doi:10.1186/1744-8069-4-61
21. Mlost J, Kostrzewa M, Malek N, Starowicz K. Molecular understanding of the activation of CB1 and blockade of TRPV1 receptors: implications for novel treatment strategies in osteoarthritis. *Int J Mol Sci*. 2018;19(2):342. doi:10.3390/ijms19020342
22. Gavenis K, Schumacher C, Schneider U, Eisfeld J, Mollenhauer J, Schmidt-Rohlfing B. Expression of ion channels of the TRP family in articular chondrocytes from osteoarthritic patients: changes between native and in vitro propagated chondrocytes. *Mol Cell Biochem*. 2009;321(1–2):135–143. doi:10.1007/s11010-008-9927-x
23. Lowin T, Tigges-Perez MS, Constant E, Pongratz G. Anti-inflammatory effects of cannabigerol in rheumatoid arthritis synovial fibroblasts and peripheral blood mononuclear cell cultures are partly mediated by TRPA1. *Int J Mol Sci*. 2023;24(1):855. doi:10.3390/ijms24010855
24. Fu M, Meng L, Ren H, Luo F. Pulsed radiofrequency inhibits expression of P2X3 receptors and alleviates neuropathic pain induced by chronic constriction injury in rats. *Chin Med J*. 2019;132(14):1706–1712. doi:10.1097/CM9.0000000000000302
25. Lee SH, Kao CC, Liang HW, Wu HT. Validity of the Osteoarthritis Research Society International (OARSI) recommended performance-based tests of physical function in individuals with symptomatic Kellgren and Lawrence grade 0-2 knee osteoarthritis. *BMC Musculoskeletal Disorders*. 2022;23(1):1040. doi:10.1186/s12891-022-06012-2
26. Aletaha D, Smolen JS. Diagnosis and management of rheumatoid arthritis: a review. *JAMA*. 2018;320(13):1360–1372. doi:10.1001/jama.2018.13103
27. Smith MH, Berman JR. What is rheumatoid arthritis? *JAMA*. 2022;327(12):1194. doi:10.1001/jama.2022.0786
28. Erdine S, Ozyalcin NS, Cimen A, Celik M, Talu GK, Disci R. Comparison of pulsed radiofrequency with conventional radiofrequency in the treatment of idiopathic trigeminal neuralgia. *Eur J Pain*. 2007;11(3):309–313. doi:10.1016/j.ejpain.2006.04.001
29. Kroll HR, Kim D, Danic MJ, Sankey SS, Gariwala M, Brown M. A randomized, double-blind, prospective study comparing the efficacy of continuous versus pulsed radiofrequency in the treatment of lumbar facet syndrome. *J Clin Anesth*. 2008;20(7):534–537. doi:10.1016/j.jclinane.2008.05.021
30. Kim YH, Lee CJ, Lee SC, et al. Effect of pulsed radiofrequency for postherpetic neuralgia. *Acta Anaesthesiol Scand*. 2008;52(8):1140–1143. doi:10.1111/j.1399-6576.2008.01752.x
31. Tanaka N, Yamaga M, Tateyama S, Uno T, Tsuneyoshi I, Takasaki M. The effect of pulsed radiofrequency current on mechanical allodynia induced with resiniferatoxin in rats. *Anesth Analg*. 2010;111(3):784–790. doi:10.1213/ANE.0b013e3181e9f62f
32. Ozsoylar O, Akcali D, Cizmeci P, Babacan A, Cahana A, Bolay H. Percutaneous pulsed radiofrequency reduces mechanical allodynia in a neuropathic pain model. *Anesth Analg*. 2008;107(4):1406–1411. doi:10.1213/ane.0b013e31818060e1
33. Gouin O, L'Herondelle K, Lebonvallet N, et al. TRPV1 and TRPA1 in cutaneous neurogenic and chronic inflammation: pro-inflammatory response induced by their activation and their sensitization. *Protein Cell*. 2017;8(9):644–661. doi:10.1007/s13238-017-0395-5
34. Atoyian R, Shander D, Botchkareva NV. Non-neuronal expression of transient receptor potential type A1 (TRPA1) in human skin. *J Invest Dermatol*. 2009;129(9):2312–2315. doi:10.1038/jid.2009.58
35. Southall MD, Li T, Gharibova LS, Pei Y, Nicol GD, Travers JB. Activation of epidermal vanilloid receptor-1 induces release of proinflammatory mediators in human keratinocytes. *J Pharmacol Exp Ther*. 2003;304(1):217–222. doi:10.1124/jpet.102.040675
36. Iannone LF, Nassini R, Patacchini R, Geppetti P, De Logu F. Neuronal and non-neuronal TRPA1 as therapeutic targets for pain and headache relief. *Temperature*. 2023;10(1):50–66. doi:10.1080/23328940.2022.2075218
37. Yuba T, Koyama Y, Uematsu H, et al. Elucidation of the treatment mechanism of pulsed radiofrequency based on its antiinflammatory effects. *Sci Rep*. 2025;15(1):33611. doi:10.1038/s41598-025-19045-z
38. Choi S, Choi HJ, Cheong Y, Chung SH, Park HK, Lim YJ. Inflammatory responses and morphological changes of radiofrequency-induced rat sciatic nerve fibres. *Eur J Pain*. 2014;18(2):192–203. doi:10.1002/j.1532-2149.2013.00391.x
39. Wang YD, Xu Y, Zhu CM, et al. Transient receptor potential channels TRPA1 and TRPV1 are involved in chronic pain relief via pulsed radiofrequency in rheumatoid arthritis rat. *Neuropharmacology*. 2025;278:110548. doi:10.1016/j.neuropharm.2025.110548